A study of multi-mode conversions in the Blackfoot 3C seismic data

Han-xing Lu and Gary F. Margrave

SUMMARY

After conventionally processing the vertical and radial components, data from the 3-C Blackfoot survey was re-processed using various flows (P-P, P-S, S-P and S-S). It was found that different energy types exist in the vertical and radial components, some of which are quite strong, while others are comparable in amplitudes to background noise. This indicates that there are multiple wave mode conversions at the earth's surface and at every interface with an impedance contrast.

INTRODUCTION

In November 1997, the CREWES recorded a 3C-2D seismic survey over the Blackfoot field, located near Strathmore, Alberta, Canada (T23 R23 W5M), where, in November 1995, a 3C-3D survey had been conducted.

Using explosives at various depths in a borehole is a common source of seismic energy. In the Blackfoot survey case, the source was 4 Kg dynamite set in a single hole at a depth of 18m, which was much less than the dominant wavelength of the reflected P-waves and S-waves. The radiated waves from this source are reflected not only from deep interfaces within the Earth, but also from the free surface. As illustrated in Figure 1, the free surface acts as a strong reflector (Aki and Richards, 1980; Fertig, 1984; Stewart, 1994).

Reflection coefficients at the free surface can be very large. In the weathering layer of the Blackfoot area, the following velocity values were obtained from data processing: Vp=610m/s, Vs=240m/s, and Vp/Vs=2.54. In order to ascertain that the incident angle was real, the ray-parameter p was restricted to the range $0<p<1/Vp$. Assuming that this is a plane wave propagating in a homogeneous media, incident on the free surface from below, the possible reflection coefficients (displacement amplitude ratios) at the free surface are shown in Figure 1. As shown in Figure 2, when an incidence ray (P-wave) reaches the free surface, it reflects as PP (P-waves) and PS (S-waves). At a large incidence angle, the reflected S-wave has a relatively strong amplitude.

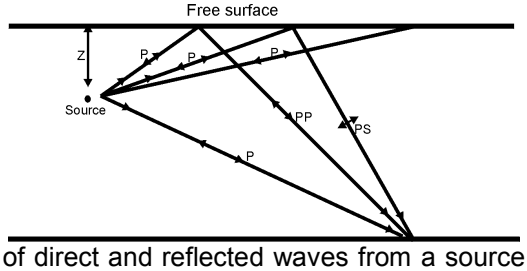

Figure 1. The ray-paths of direct and reflected waves from a source at depth z: direct wave, P; reflected P-waves, PP; and reflected S-waves, PS.

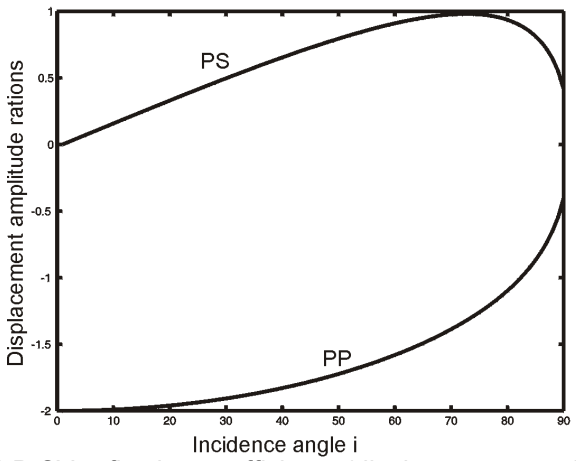

Figure 2 The P-P and P-SV reflection coefficients (displacement amplitude ratios) for a free surface with *Vp*=610m/s, *Vs*=240m/s for the weathering layer. The ray-parameter was restricted to the range 0<*p*<1/*Vp* to make sure that the incidence angle was always real.

In recent years, three component (3C) recording with a 'P-wave source' has demonstrated that both P- and S-waves can be recorded simultaneously. Shear waves are found mostly on the horizontal components. In acquiring this type of data, some adjustment of acquisition parameters is usually required (Lawton, 1993, 1994).

When processing multi-component seismic data, simple assumptions are commonly made:

(1) For vertical component data, the incident wave is P (compressive) and the reflected wave is P, no mode conversion occurs at any interface or at the free surface;

(2) For radial component data, the incident wave is P, and the recorded wave is S (shear), which has been reflected from a target interface. No mode conversion occurs at any other interface between this target and the surface, and no mode conversion occurs at the free surface (Figure 3).

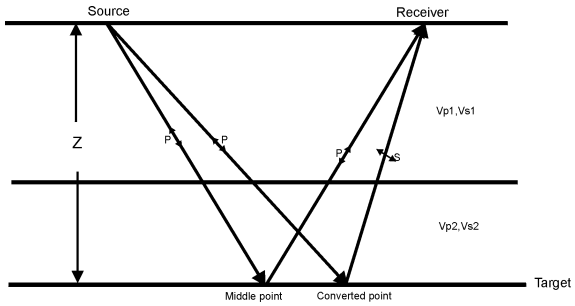

Figure 3. The assumed ray-paths for vertical and radial components when processing multi-component data.

Besides the conventional processing for P-P and P-S waves, a particular component (radial or vertical) can be processed for a specific wave-type (PP, PS, SP or SS) by simply adjusting the appropriate traveltime dependent steps. For example: to process the vertical component for SP reflections, we must apply shear-wave source statics, P-wave receiver statics, and an S-P NMO correction (with a CCP shift towards the source).

PRELIMINARY RESULTS FROM BLACKFOOT 3C-3D DATA

The 1995 Blackfoot 3C-3D data was reprocessed using conventional methods (Harrison 1992). The processing flows used have been published in the 1998 CREWES Research Report. The migrated sections for both vertical and radial components are shown in Figure 4. The time scale of the radial section was stretched for comparison with the vertical section. When processing, an average ratio of *Vp/Vs* =2.2 was used for radial component binning. We can see in Figure 4 that the events in the vertical component section tie with those in radial component quite well.

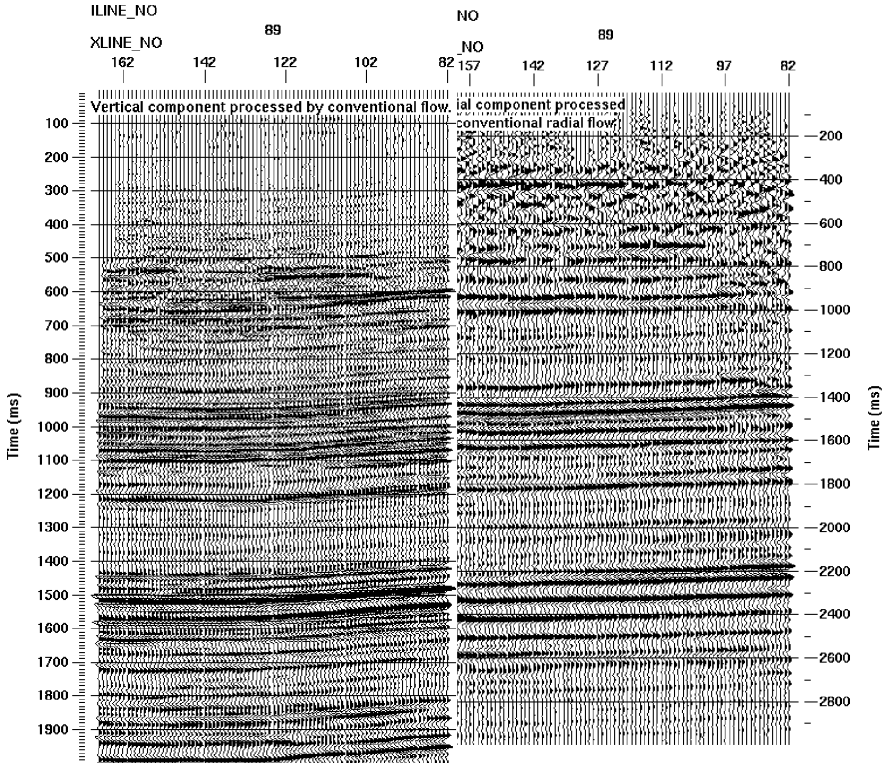

Figure 4. Stacked sections for vertical and radial components reprocessed by conventional processing flows.

Figure 5(a) shows the results from vertical component geophone records using a P-S processing flow, which is conventionally used for the radial component (Figure 5(b)). In this flow, we use the asymptotic conversion point (ACP) binning to construct the CDP gathers, and applied shear wave statics for receivers, then use the P-S stacking velocities for normal moveout correction. Comparing Figures 5(a) and (b), we can see that some vertical component events tie to events in the radial component.

In the vertical component data, we observe a small percentage of PS-wave energy. To account for this, one possibility is that there is another mode conversion at the near surface (Figure 6). More likely, it is simply that oblique S-wave arrivals are recorded in both horizontal and vertical channels because emergent angles are not exactly 90 degrees to surface.

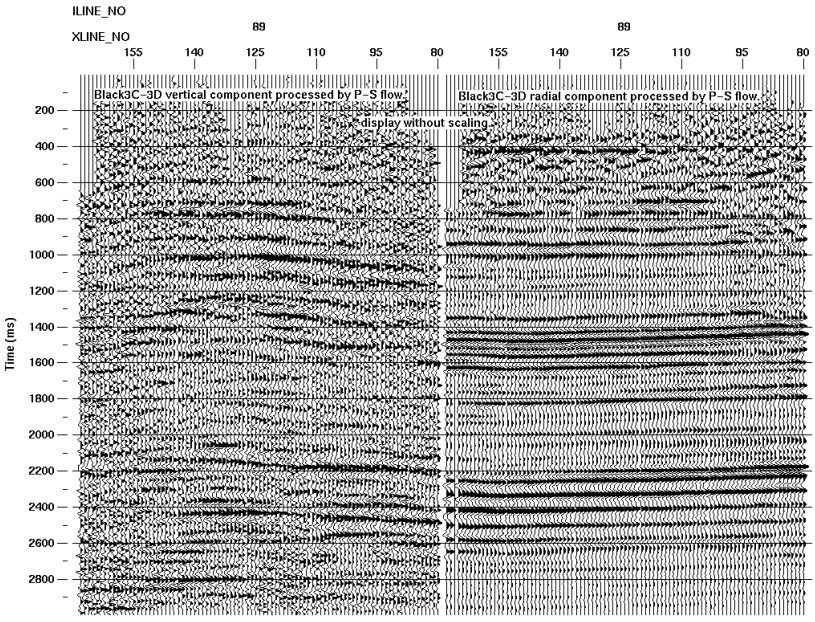

a b

Figure 5. (a) Stacked section from the vertical component and (b) a stacked section from the radial component, both using a P-S processing flow

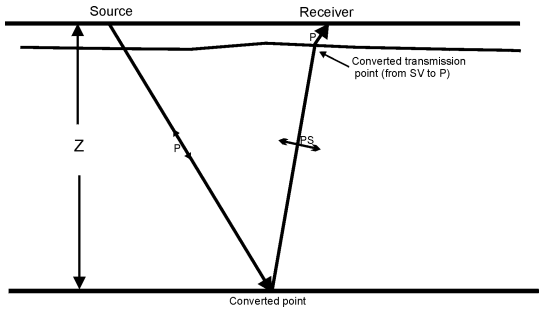

Figure 6. Possible ray-paths to account for the S-wave energy evident in vertical records. The SV-wave converts back to a P-wave at the near surface.

Figure 7(a) shows the results for the radial component processed using the P-P flow for the 1995 Blackfoot 3C-3D data. Figure 7(b) shows the stacked results for vertical component data processed conventionally using the same flow. In this flow, we use the regular mid-point binning, apply the P-wave source and receiver statics, and use the P-P stacking velocity for NMO. Again, it is possible that there is a mode conversion near the surface (Figure 8).

The result of the radial component processed using the P-P flow is different from the previous case. Here it seems that there is less energy at the same events as observed in the vertical component. We can treat these energies as background noise.

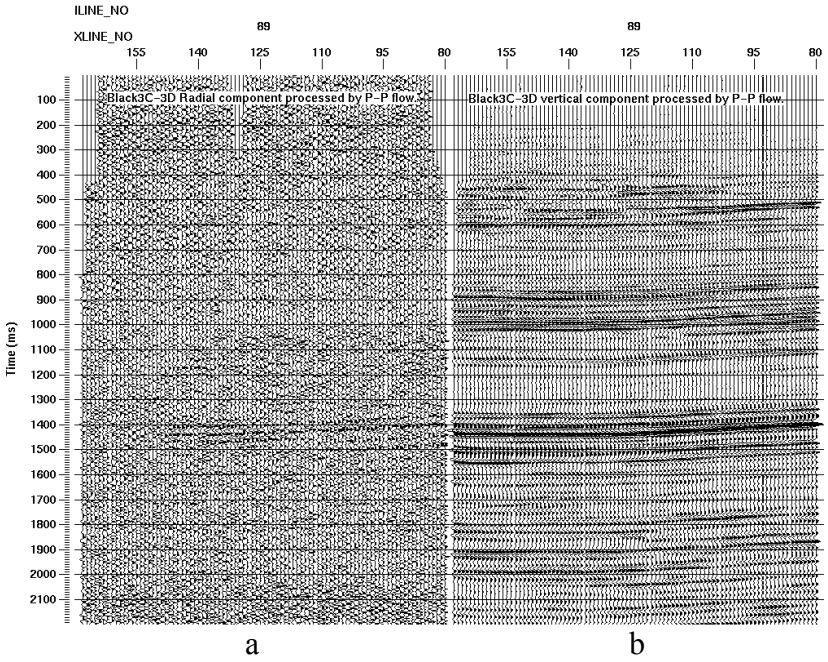

Figure 7. (a) Stacked section for radial component processed by P-P flow. (b) Stacked section for the vertical component data from the Blackfoot 3C-3D

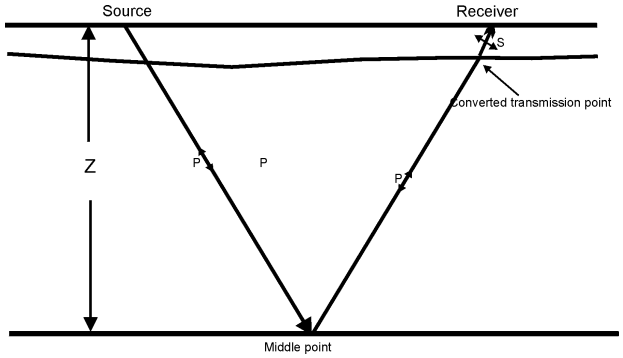

Figure 8. Possible ray-paths to account for the existence of P-wave energy in the S-wave recording.

In order to test for anisotropy and birefringence in the radial components, limited azimuth stacks were computed for the radial data. The stacked sections of all azimuths, and 110 and 280 degrees of source-receiver azimuths for the radial component, are shown in Figure 9. There is no strong evidence of anisotropy or birefringence.

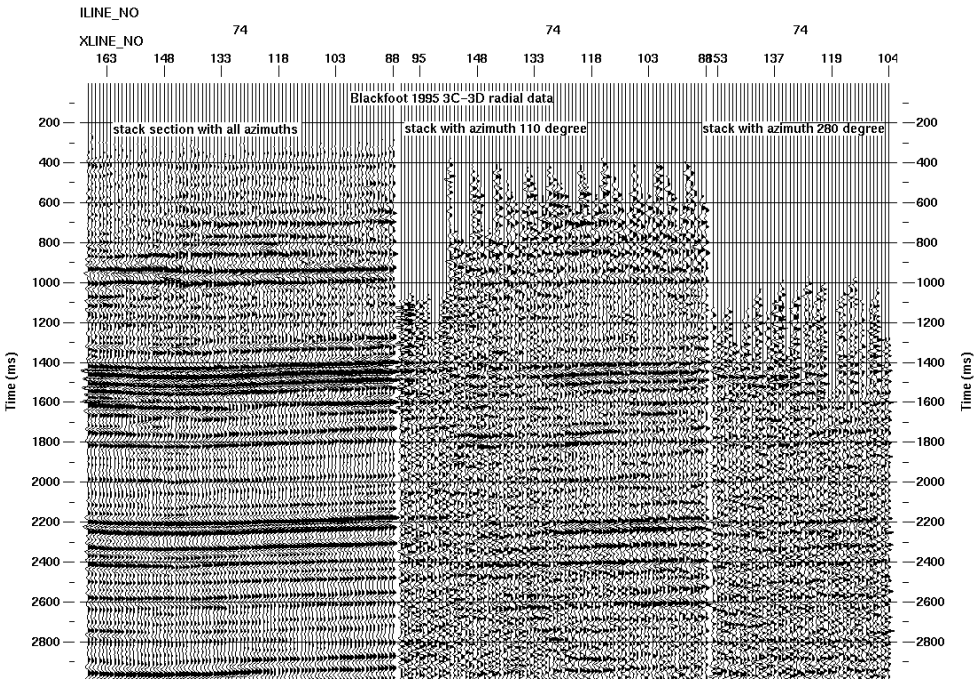

Figure 9. Stacked sections of different azimuths for the radial component from the 1995 Blackfoot 3C-3D data.

PRELIMINARY RESULTS FROM BLACKFOOT 3C-2D DATA

Similar experiments were performed on the 1997 Blackfoot 3C-2D data. The raw data was recorded using vertical, horizontal-north and horizontal-east geophones. The raw shot gathers, after 3-component reorientation (geometrical rotation for horizontal records only), are shown in Figure 10 as vertical, radial and transverse components.

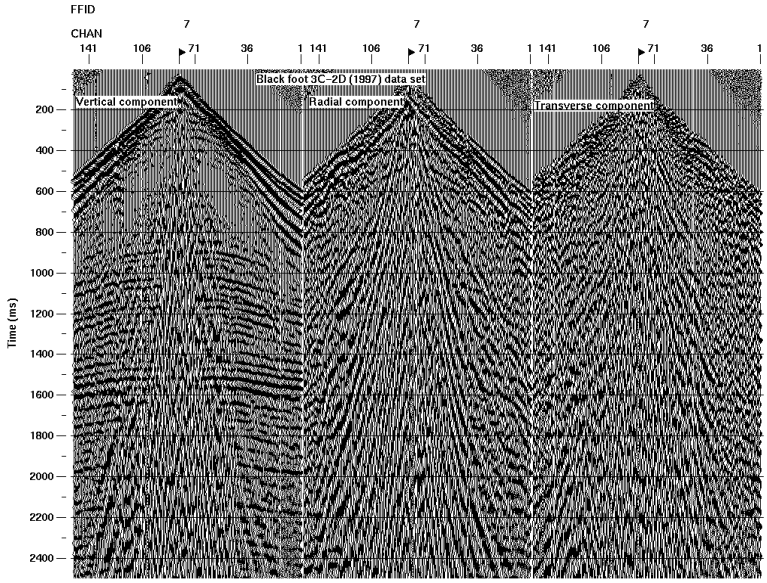

Figure 10. Raw shot gathers after 3-component reorientation: vertical component (left); radial component (centre); and transverse component (right).

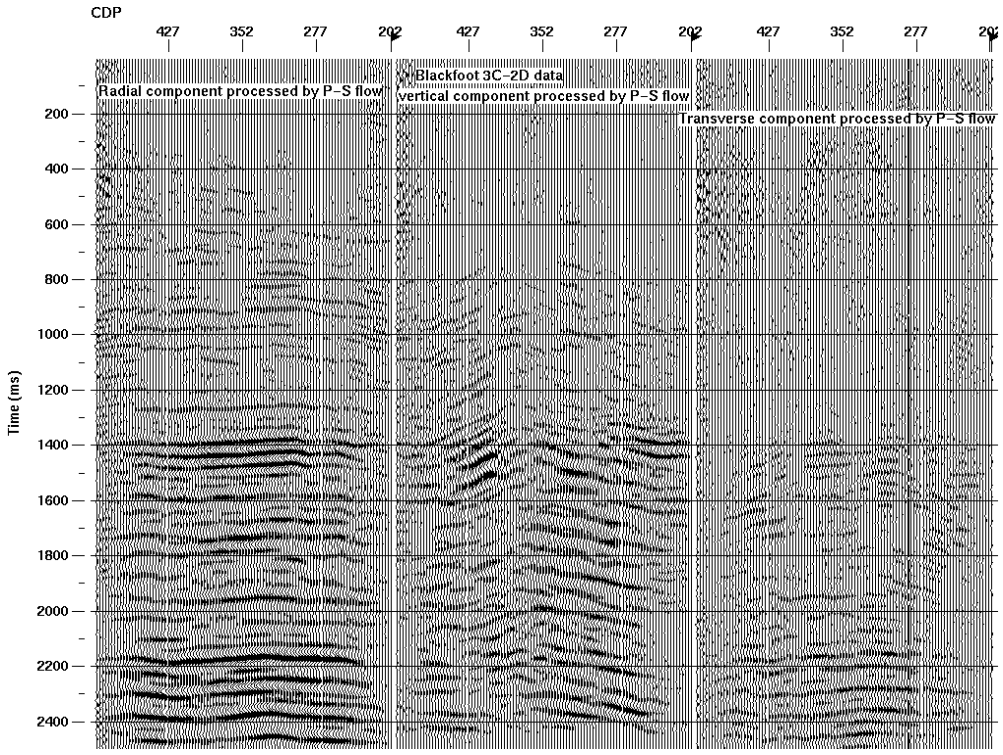

Figure 11. Stacked sections using the same P-S flow: (left) results of the radial component; (centre) vertical component; and (right) transverse component.

The stacked sections for radial, vertical and transverse components processed using the same P-S flow are shown in Figure 11. The amplitude for the transverse component was multiplied by 20 for the purposes of comparison. Here we can see that in the 1997 Blackfoot 3C-2D case, after geometrical rotation for H-north and H-east, coherent but weak SV-wave energy is present in the transverse component. The image of the S-wave seen in the vertical data is interesting and bears further investigation.

The radial and transverse components were also processed with a S-S flow. In this flow, we changed polarities for negative offsets, used mid-point binning, applied shear-wave statics for shots and receivers, used S-S stacking velocities generated from P-P velocities (from the *Vp/Vs* ratios in different time window) for NMO.

The results are shown in Figure 12. Note that the time scale was stretched for comparison with the vertical results. The energies are very weak compared with the amplitude of the vertical component and can also be treated as background noise.

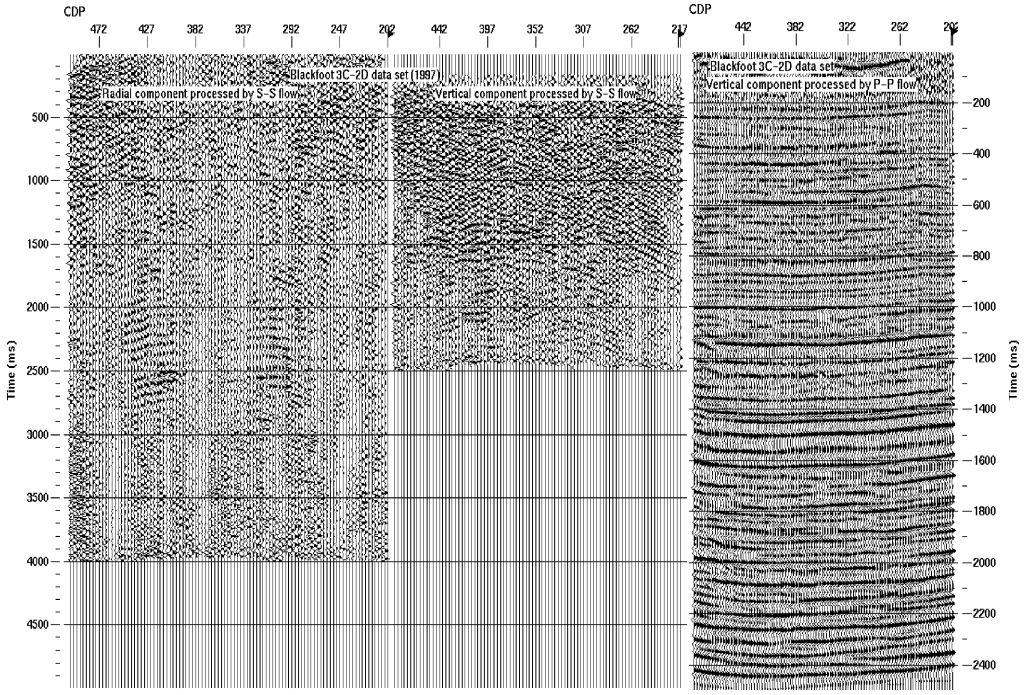

Figure 12. The stacked sections for radial and transverse components processed by S-S flow compared with vertical component processed by P-P flow.

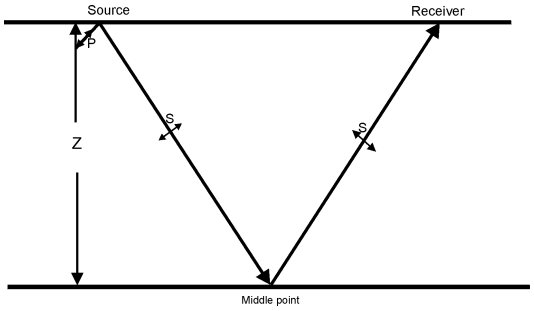

Figure 13. Assumed ray-path for S-S processing flow.

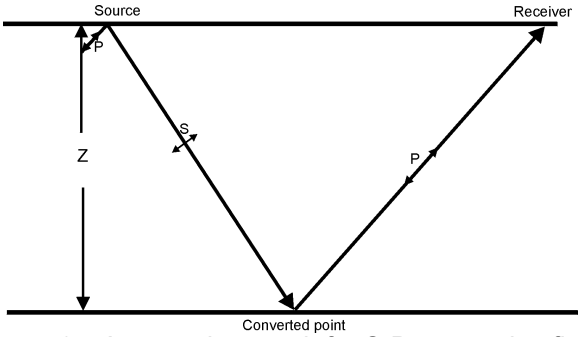

Figure 14. Assumed ray-path for S-P processing flow.

We also processed the vertical component with an S-P flow. This used *Vs/Vp*=0.5 for ACP binning which moved to conversion point toward source, shear-wave statics for shots and *Vs-Vp* stacking velocities, which are the same as the P-S stacking velocities for NMO. No polarity change was introduced on the negative offsets because the data was supposed to be recorded on vertical geophones. The stacked section is shown in the middle panel of Figure 15. In this case, an apparent S-P mode-converted wave can be seen in the stacked section, especially in the time window between 700ms-1400ms. The energy of the P-S mode-converted wave is relatively strong at 1400ms-2400ms. Currently, the reason for these differences is unknown.

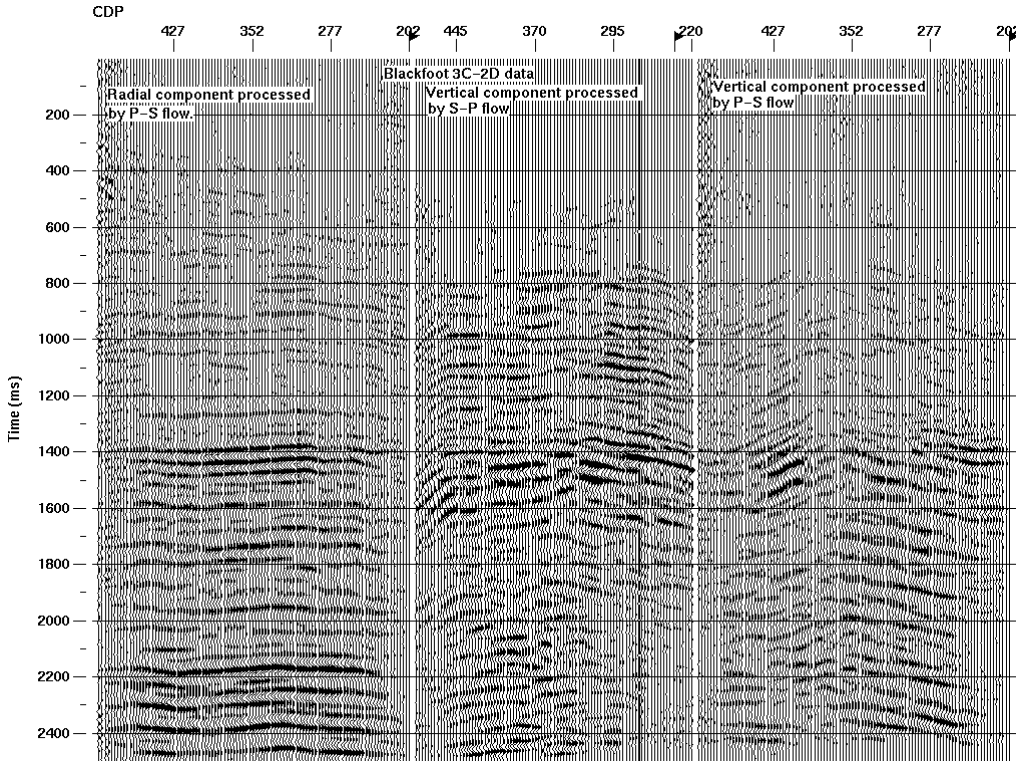

Figure 15. Stacked section for radial component processed by P-S flow (left); stacked section for vertical component processed by S-P flow (centre); stacked section for vertical component processed by P-S flow (right).

The radial component was processed with S-P processing flow (Figure 16, centre), and with P-P flow (vertical component conventional flow: Figure 16, right). The P-wave energies recorded in the radial component are relatively moderate, especially those reflections from the basement. They are at about 2200ms in the P-S or S-P sections, and at about 1400ms in the P-P sections. The time scale of the P-P seismic section (Figure 16, right) was stretched for comparison with the result of the radial component.

The sections on the left and in the middle are obtained using the same values as the velocity function. However, they have a different physical meaning. The P-S velocity is the stacking velocity function of the downgoing P-wave and the upgoing S-wave. The S-P velocities are the stacking velocity function of the downgoing S-wave and the upgoing P-wave. Again, the false structures evident on these sections bear further investigation.The result in Figure 16 (right) indicates this on the radial component. It

contains some percentage of P-P wave energy. This might be recorded by horizontal geophones because of the non-vertical emergent rays. If this is the case, the P-P and P-S waves could be separated by the maximum power method.

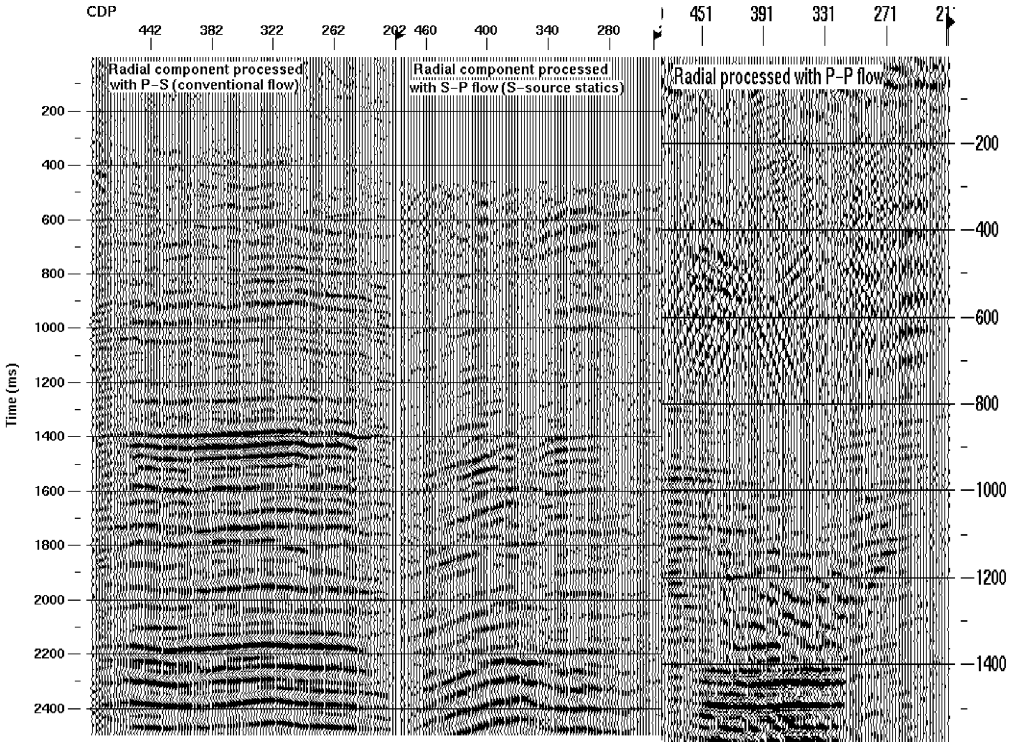

Figure 16. The stacked section for the radial component processed with a conventional processing flow is on the left, the stacked section for the radial component with an S-P flow is in the middle, the stacked section for the radial component with a P-P flow on the right. The time scale was stretched to match the reflections.

From Figure 17(a), the near-surface ray-paths for a P-wave source can be one of two cases. The first is downgoing P-wave which, at some interface in the near surface, converts to an S-wave. The S-P flow was used for processing in this case, except that the P-wave source statics were applied to the source.

In Figure 17(b), the P-wave reached the free surface, then reflected as an S-wave. In this case, when we processed the data, the S-P flow was used except that P+S-wave statics were applied to the sources.

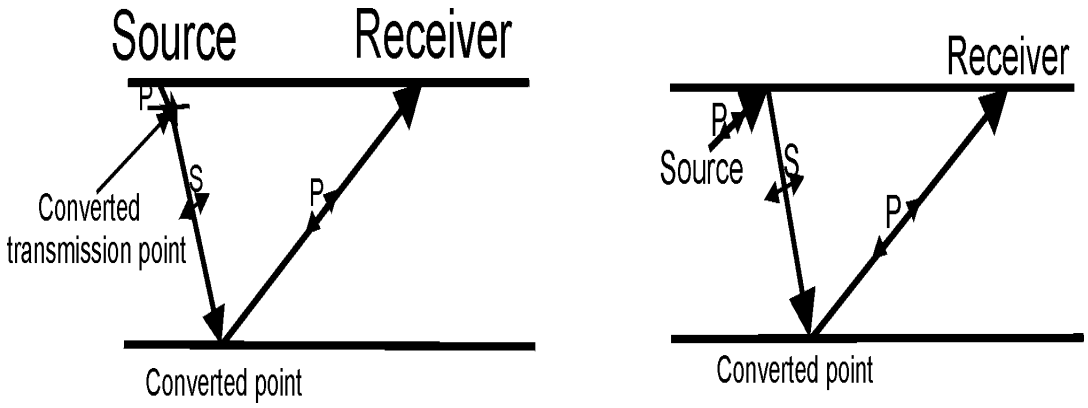

Figure 17. Ray-paths for two different cases are shown. The reflected P-wave is recorded a the receiver.

The results are shown in Figure 18. The energies in the stacked sections with P-wave and P+S wave source statics applied, are relatively strong in the coal formations at approximately 1400ms. The energies are very weak in the Glauconitic channel, which lies just below 1600ms. We currently cannot explain this false structure.

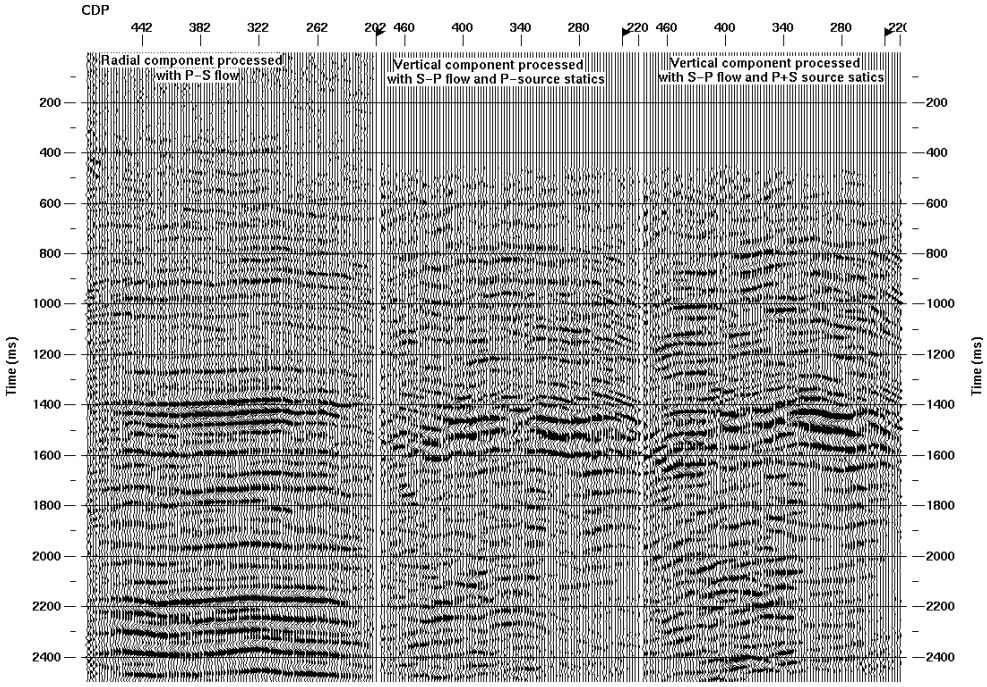

Figure 18. The stacked section for the radial component processed using the conventional P-S flow (left); the stacked section for the vertical component processed using the S-P flow with the P-wave source statics (centre); the stacked section for the vertical component processed using the S-P flow with the P-wave and S-wave source statics (right).

A more accurate 3C orientation is obtained using Maximum Power analysis to get vertical, radial and transverse components. It means that not only the horizontal components need to be geometrically rotated. All three components are used to

project the maximum power onto the vertical component. Power that cannot be projected onto the vertical component is maximized on the radial component. Any energy not projected onto either the vertical or radial components is projected onto the transverse component. In this way we get more pure mode energy in these three components, but we still cannot get the multi-converted components (PSP, SPS, SP et.). This test will be subject to future research.

DISCUSSION

Propagation of elastic waves in the earth is much more complicated than our simple processing flows assume. An compressive wave incident at an interface between two solid media has four scattered waves (Figure 19). As a result of the numerous possibilities of multiple mode conversions, there are many possible mode-converted arrivals (P-P, P-S, S-P, S-S, P-S-P etc.) at the geophones on the surface.

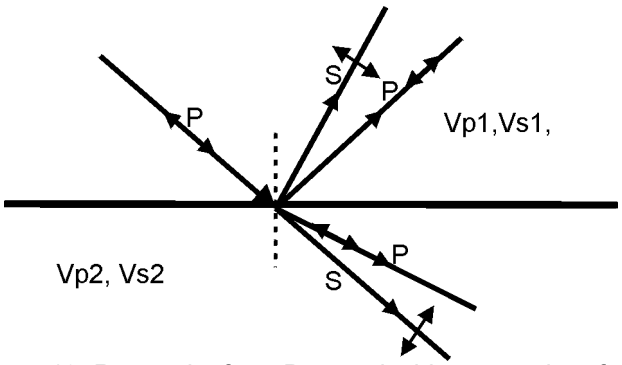

Figure 19. Ray-paths for a P-wave incident at an interface.

Due to the receiving characteristics of the geophones, P- and S- waves are recorded on both horizontal and vertical geophones (Dankbaar 1985). What we should do is to remove the effect of the geophones receiving characteristics and find the true amplitudes of P-waves and S-waves arriving at the earth's surface.

The emergent ray is not exactly perpendicular to the earth's surface. This is probably caused by non-zero-offset reflections or refractions. The magnetic leakage between the components of 3-C geophones may cause additional mode leakage.

ACKNOWLEDGEMENTS

We would like to thank the sponsors of the CREWES project for their financial support. We also thank our colleagues at CREWES for their assistance in this project.

REFERENCES

Aki. K. and Richards, P. G. 1980, Quantitative seismology, Theory and Methods, Vol. 1, W.H.Freeman, San Francisco.

Fertig, J., 1984, Shear waves by an explosive point-source: the earth surface as a generator of converted P-S waves. Geophysical Prospecting 32, 1-17.

Dankbaar, J.W.M., 1985, Separation of P- and S-waves, Geophysical Prospecting 33, 970-986.

Harrison, M.P., 1992, Ph.D. Thesis: Processing of P-SV surface-seismic data: Anisotropy Analysis, Dip Moveout, and Migration, The University of Calgary, Department of Geology and Geophysics.

Lawton, D.C. 1993, Optimum bin size for converted-wave 3-D asymptotic mapping: CREWES Project, Annual Research Report, Volume 5, 28.1-28.16.

Lawton, D.C. 1994 Acquisition design for 3-D converted waves: CREWES Project, Annual Report, Volume 6, 23-1-23.23.

Stewart R.R., 1994 The present and promise of P-S seismic exploration: CREWES Project, Annual Research Report, Volume 6, 1.1-1.31